

vents. Thus, treatment of **2** with perdeuterated ethanol forms only **7**, in which the alkoxy group has been exchanged but the hydrido ligand has not.

The insertion chemistry of this complex also differs from that of other, more common, group 8-10¹¹ alkyl- and hydridometal complexes. Dative ligands such as CO and ethylene do not promote insertion (see above), and **2** catalyzes decomposition of (trimethylsilyl)ketene. However, insertion does take place with more electrophilic reagents such as CO₂ and CS₂, leading to the metallacarbonate Cp*(L)(H)Ir-O-C(O)-OEt (**11**; 78% by NMR) and the corresponding xanthate **12** (58%, isolated).⁸ Note that this transformation involves only the metal-oxygen bond; no insertion into the M-H bond is observed.⁹ The CO₂ insertion product **11** is thermally unstable in solution and as a solid and therefore has been characterized only by ¹H NMR and IR spectroscopy. The metallaxanthate **12**, however, is stable indefinitely as a solid at room temperature under a nitrogen atmosphere and has been fully characterized.⁶

Preliminary studies of the mechanisms of the PPh₃-induced (apparent) reductive elimination and CS₂ insertion reactions have been carried out. Unlike reductive elimination of Cp*(PMe₃)₂Ir(R)(H)^{4d}, the rate of disappearance of **2** is dependent upon the concentration of added trapping reagent (PPh₃). Typical saturation kinetics are observed; when excess phosphine is used, at low absolute concentrations of added ligand, the pseudo-first-order rate constant *k*_{obsd} increases with increasing [PPh₃], but it levels off to a maximum *k*_{obsd} of 5.7 × 10⁻⁴ s⁻¹ at high concentrations. This requires the reversible formation of a reactive intermediate that can be trapped by phosphine; at high [PPh₃] it is trapped essentially every time it is formed. The complete absence of cyclometallation product **3** or hydridophenyl complex **4**, even in benzene solvent, makes it very unlikely that this intermediate is the earlier-identified C-H activating species Cp*Ir(PPh₃). Similar kinetic studies carried out on the CS₂ insertion reveal no dependence of *k*_{obsd} on the concentration of CS₂. Thus once again an intermediate capable of being trapped by the added reagent is implicated, except in this case return of the intermediate to **2** is too slow to compete with the trapping step. Significantly, the value of *k*_{obsd} for the CS₂ insertion is 7.2 × 10⁻⁴ s⁻¹, very similar to the limiting value of *k*_{obsd} for the reaction induced by phosphine.

The similarity of these limiting rate constants provide strong evidence that the two reactions, despite their apparent overall dissimilarity, proceed through the same intermediate, indicated as **13** in Scheme I. Three possible structures for this intermediate (**13a-c**) are illustrated at the bottom of the scheme. Additional data provided insight into the nature of **13**. Kinetic studies on the maximum rate (where *k*_{obsd} = *k*₁) of reaction of PPh₃ with **2**, in which the metal-bound hydrogen has been replaced with deuterium, reveal that the process occurs with [*k*_H/*k*_D] = 1. This lack of an isotope effect confirms the absence of a direct reductive elimination to either free or coordinated ethanol and argues against mechanisms that involve M-H bond cleavage in the rate-determining step (e.g., reversible transfer of hydrogen to the Cp* ring). Kinetics carried out in dimethylformamide again show no dependence on [PPh₃] at high concentrations of entering ligand and give *k*₁ = 3.6 × 10⁻⁴ s⁻¹, very close to the rate constant measured in toluene. This argues strongly against ion pair intermediate **13a**, which should be formed at a much higher rate in the more polar solvent.¹⁰ We conclude that the intermediate is an uncharged,

coordinatively unsaturated species, perhaps formed by either "slippage" of the Cp* ring (**13b**) or direct transfer of the alkoxy group to this ring (**13c**). Experiments are now under way aimed at distinguishing these possibilities.

In summary, hydridoalkoxyiridium hydrides can be prepared but are quite reactive; their chemistry is substantially different from that of early or higher valent metal alkoxides. Further reactions of these materials, as well as additional information on the mechanism of the reactions summarized here, will be reported in a full paper.

Acknowledgment. We gratefully acknowledge Dr. Mark D. Seidler for helpful discussions. We also appreciate helpful discussions with Drs. H. E. Bryndza and J. D. Atwood, as well as their willingness to disclose results prior to publication. Financial support for this work was provided by the National Institutes of Health (Grant GM25459).

Supplementary Material Available: Spectral and analytical data for **2**, **6-8**, and **10-12** (3 pages). Ordering information is given on any current masthead page.

(11) In this paper the periodic group notation is in accord with recent actions by IUPAC and ACS nomenclature committees. A and B notation is eliminated because of the wide confusion. Groups IA and IIA become groups 1 and 2. The d-transition elements comprise groups 3 through 12, and the p-block elements comprise groups 13 through 18 (Note that the former Roman number designation is preserved in the last digit of the new numbering: e.g., III → 3 and 13.)

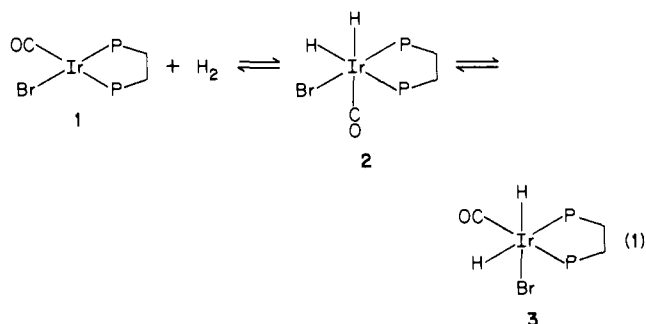
Diastereoselection and the Influence of Chiraphos on Metal-Centered Chirality in Cis Oxidative Addition of Hydrogen and Triphenylsilane

Amanda J. Kunin, Ramy Farid, Curtis E. Johnson, and Richard Eisenberg*

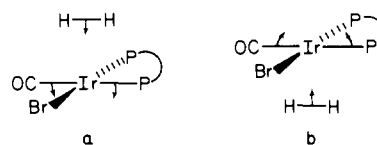
Department of Chemistry, University of Rochester
Rochester, New York 14627

Received May 6, 1985

In the stereoselective, kinetically controlled oxidative addition of H₂ to IrBr(CO)(dppe) (**1**) (dppe = bis(diphenylphosphino)ethane),¹ both the kinetic isomer **2** and the thermodynamic isomer **3** form as racemates resulting from H₂ approach to the metal



center from above and below the Ir(I) square-planar complex. This is illustrated for **2** as a and b with H₂ aligned parallel to the



(1) (a) Johnson, C. E.; Fisher, B. J.; Eisenberg, R. *J. Am. Chem. Soc.* **1983**, *105*, 7772. (b) Johnson, C. E.; Eisenberg, R. *J. Am. Chem. Soc.* **1985**, *107*, 3148.

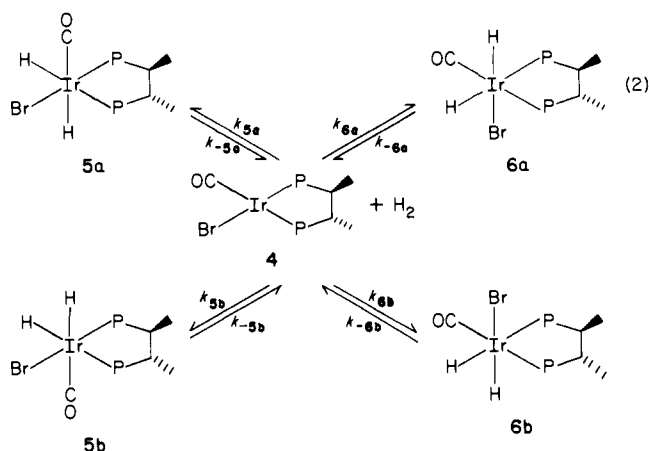
(8) A referee has pointed out that metal alkyls often insert CS₂ to give M-CS₂R rather than M-S-C(S)R complexes and asked how we ruled this out in the case of **12**. This type of insertion seems particularly unlikely in our case, since it would lead to the formation of an S-O bond in M-C(S)S-OR. However, experimental evidence is supplied by the lack of phosphorus-carbon coupling to the sulfur-bound carbon in the ¹³C NMR spectrum; a typical value for this coupling constant in iridium complexes that do have a P-M-C linkage is 13 Hz.

(9) For example of CO₂ and CS₂ insertion into a metal-hydrogen bond, see: (a) Butler, A. S.; Fenster, A. E. *J. Organomet. Chem.* **1974**, *66*, 162. (b) Volpin, M. E.; Kolomnikov, I. S. *Organomet. React.* **1975**, *5*, 313.

(10) As discussed in ref 1d, a cationic iridium/anionic methoxide ion pair has been postulated as an intermediate in the carbonylation of the 16-electron complex MeOIr(CO)(PPh₃)₂; however, a similar platinum alkoxide CO insertion is thought not to proceed via ionic intermediates.²

P–Ir–CO axis of complex **1**; formation of **3** proceeds similarly with H₂ parallel to P–Ir–X. In this paper, we describe studies in which the optically active diphosphine chiraphos ((2*S*,3*S*)-bis(diphenylphosphino)butane)² is used in place of dppe leading to kinetic and thermodynamic differentiation of the racemic products of H₂ and Ph₃SiH oxidative addition. While the use of chiral diphosphines as catalysts for asymmetric hydrogenation has been widely investigated,^{3,4} the present work represents the first study in which the effect of chiraphos on simple oxidative addition has been examined.

The complex IrBr(CO)(chiraphos) (**4**), prepared analogously to **1**,^{1a} reacts with H₂ in acetone similarly to eq 1 forming first diastereomers **5a** and **5b** with >99.5% stereoselectivity followed by slower formation of the more stable pair of diastereomers **6a** and **6b**. Figure 1 shows the hydride region of the ¹H NMR spectrum upon initial oxidative addition and subsequent isomerization, and NMR data for the diastereomers are summarized below.⁵ At –25 °C, the kinetic diastereomers **5** form in a 2.1:1 ratio which remains constant for extended periods of time but, on warming to room temperature, changes within 5 min to 1.2:1 as the thermodynamic diastereomers **6** start to grow in. The



isomerization of **5** to **6** follows first-order kinetics with a rate constant for the disappearance of **5a** at 35 °C of $4.9 \times 10^{-5} \text{ s}^{-1}$. During early stages of the isomerization the observed ratio **6a:6b** is 2.4:1, while at equilibrium the ratio is 1.3:1 with diastereomers **6** comprising 85% of the total hydride species present. At equilibrium, the ratio **6a:5a** is 7.2:1.

To establish that the initial ratio of 2.1:1 seen for **5** at –25 °C corresponds to kinetic differentiation of the diastereomers, **5** was formed at low temperature followed by replacement of H₂ by D₂. After 1 h at –25 °C the amount and ratio of diastereomers of **5** showed no change, but upon warming to room temperature the hydride resonances rapidly diminished and disappeared within 1 h, following first-order kinetics with a rate constant of $3.3 \times 10^{-3} \text{ s}^{-1}$ for diastereomer **5a**.

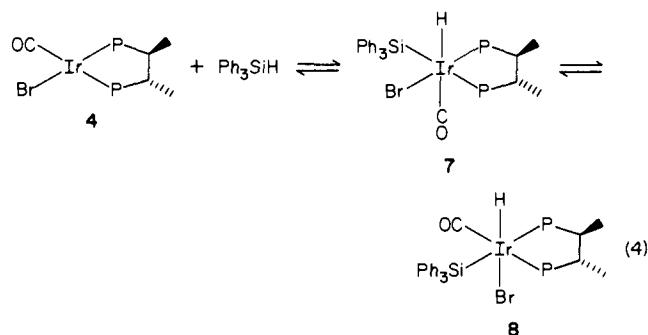
The experiments outlined above show that in addition to the stereoselective, kinetically controlled H₂ oxidative addition originally seen in eq 1, diastereoselection for **5** and **6** occurs due solely to the influence of chiraphos on the developing chirality at the metal center as the cis oxidative addition proceeds. The kinetic differentiation expressed as $\Delta\Delta G^\ddagger$ for **5a/5b** and **6a/6b** is 0.40

and 0.50 kcal/mol, respectively. From the experiment under D₂, we see that reductive elimination of H₂ from **5** is rapid at room temperature, indicating that equilibrium between **5a** and **5b** is established prior to isomerization to **6** and suggesting that the mechanism for isomerization involves reductive elimination to generate **4** followed by oxidative addition with H₂ parallel to P–Ir–X forming **6**. The proposed mechanism is shown as eq 2.⁶ From the initially observed ratio of >200:1 for **5/6** and eq 3, we

$$\frac{[\mathbf{5a} + \mathbf{5b}]}{[\mathbf{6a} + \mathbf{6b}]} = e^{-(\Delta G^\ddagger_{5a} - \Delta G^\ddagger_{6a})/RT} \frac{(1 + k_{5b}/k_{5a})}{(1 + k_{6b}/k_{6a})} \quad (3)$$

conclude that $\Delta\Delta G^\ddagger$ between the formation of **5a** and **6a** must be >3.1 kcal/mol. The thermodynamic differentiation between the diastereomers is obtained from the ratio **5a:5b** as **6** starts to form, and the ratios **6a:6b** and **6a:5a** after equilibrium has been reached. A reaction coordinate profile of the **4** + H₂ system summarizing all of these results is given in Figure 2.

The oxidative addition of Ph₃SiH to **4** also proceeds stereoselectively under kinetic control in agreement with recent observations for silane addition to complex **1**.⁷ The reaction occurs as shown in eq 4 with the initial formation of **7** (>99.5%) followed



by isomerization to the more stable diastereomers **8**.⁸ The kinetic differentiation for **8** is striking as evidenced by the ratio **8a:8b** of 12:1 during early stages of the isomerization, corresponding to $\Delta\Delta G^\ddagger$ of 1.5 kcal/mol for the formation of the diastereomers. The eventual ratio **8a:8b** at equilibrium is 1:1 indicating little thermodynamic differentiation between the diastereomers.

The isomerization of **7** to **8** most probably occurs by reductive elimination/oxidative addition similar to that shown in (2) since the reaction follows first-order kinetics and reductive elimination of Ph₃SiH from **7** is rapid relative to isomerization. The latter was shown by preparing **7** at –20 °C followed by the addition of **5** equiv MeCl₂SiH which acts as an efficient trap for **4** by its oxidative addition to form IrHBr(SiMeCl₂)(CO)(chiraphos). Further studies using these and other silanes will be reported separately.

(6) The assignment of metal-centered chirality for all of the diastereomers is based on an analysis of space-filling models of reactants and products for the oxidative addition reaction. These models, which are particularly informative for the silane oxidative addition, predict a kinetic preference for the Δ configuration in the formation of both **5** and **6** and little thermodynamic differentiation within each pair of diastereomers. These predictions must, of course, be confirmed by X-ray structural studies. A different analysis has been presented by Brown and Chaloner who propose that diastereoselection of H₂ oxidative addition to Rh(α -benzamidoacetic acid)(chiraphos)⁺, which was not observed directly, is determined by torsional strain in the Rh–chiraphos chelate ring. Brown, J. M.; Chaloner, P. A. In "Homogeneous Catalysis with Metal Phosphine Complexes", Pignolet, L., Ed.; Plenum Publishing: New York, 1983; 161–162. However, the importance of electron factors in determining the diastereoselection in the Rh(chiraphos) system has not been examined as it has for IrBr(CO)(dppe).¹

(7) Johnson, C. E.; Eisenberg, R. *J. Am. Chem. Soc.*, in press.

(8) ¹H NMR data for hydride resonances in acetone-*d*₆ (*J*_{PH} in Hz). **7a**: –7.93 (dd, 16.8, 12.6). **7b**: –8.49 (dd, 24.2, 13.7). **8a**: –16.04 (dd, 13.7, 7.4). **8b**: –16.34 (dd, 24.2, 5.3). Molecular models indicate that the configuration at the metal for diastereomer **8a** which is kinetically preferred over **8b** is Δ .

(2) Fryzuk, M. D.; Bosnich, B. *J. Am. Chem. Soc.* **1977**, *99*, 6262.

(3) (a) Knowles, W. S.; Sabacky, M. J.; Vineyard, B. D. *Adv. Chem. Ser.* **1974**, *132*, 274. (b) Kagan, H. B. *Pure Appl. Chem.* **1975**, *43*, 401 and references therein. (c) Valentine, D. S.; Scott, J. W. *Synthesis* **1978**, 329. (d) Bosnich, B.; Roberts, N. K. *Adv. Chem. Ser.* **1982**, *196*, 337. (e) Brown, J. M.; Chaloner, P. A.; Parker, D. *Adv. Chem. Ser.* **1982**, *196*, 355.

(4) (a) Chan, A. S. C.; Pluth, J. J.; Halpern, J. *J. Am. Chem. Soc.* **1980**, *102*, 5952. (b) Brown, J. M.; Chaloner, P. A. *J. Chem. Soc., Chem. Commun.* **1980**, 344. (c) Chua, P. S.; Roberts, N. K.; Bosnich, B.; Okrasinski, S. J.; Halpern, J. *J. Chem. Soc., Chem. Commun.* **1981**, 1278.

(5) ¹H NMR data for hydride resonances in acetone-*d*₆ (*J*_{PH} in Hz). **5a**: –8.85 (dd, 14.7, 12.9), –9.25 (dd, 21.6, 16.7). **5b**: –9.02 (dd, 14.5, 12.9), –9.28 (~t, 20.8). **6a**: –8.71 (ddd, 127.1, 15.7, 4.3), –18.0 (mult). **6b**: –9.50 (ddd, 128.8, 16.7, 4.9), ~–18.1 (mult).

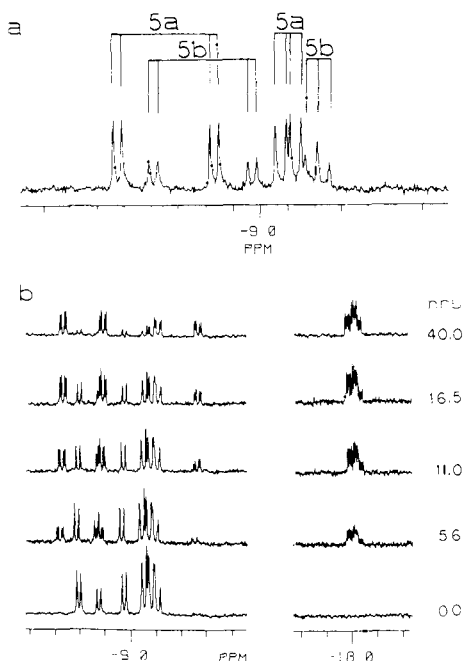


Figure 1. Hydride region of the ^1H NMR spectrum of $\text{IrBr}(\text{CO})(\text{chiraphos})$ (**4**) plus H_2 in acetone- d_6 : (a) expanded view at -25°C ; (b) spectra taken over 40-h period monitoring the conversion from diastereomers **5** to **6** at 25°C .

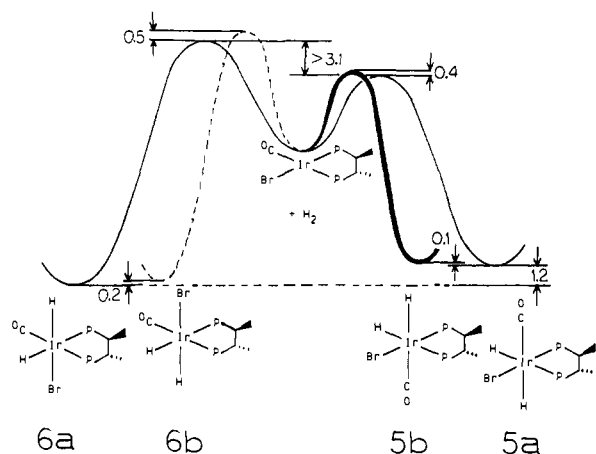


Figure 2. Reaction coordinate diagram for the system $\text{IrBr}(\text{CO})(\text{chiraphos})$ (**4**) + H_2 . Values of $\Delta\Delta G$ and $\Delta\Delta G^\ddagger$ are given in kcal/mol.

The results described above show that kinetic and thermodynamic differentiation of metal-centered chirality in simple cis oxidative additions by chiraphos is significant.⁹ The results also provide a sensitive probe to the transition-state structure in these systems through observed differences in the extent of kinetic and thermodynamic differentiation for the diastereomers in these cis oxidative additions. On the basis of these differences, it appears that for both H_2 and Ph_3SiH oxidative addition, the transition state in these reactions is not very product-like.

Acknowledgment. We thank the National Science Foundation (CHE 83-08064) and the Office of Naval Research for support of this work and Johnson Matthey Co., Inc., for a generous loan of iridium salts.

(9) (a) While diastereomeric cis dihydrides have been seen previously for $[\text{IrH}_2(\text{dipamp})_2]\text{BF}_4$, the stereoselectivity of the oxidative addition was not reported. Brown, J. M.; Dayrit, F. M.; Lightowler, D. *J. Chem. Soc., Chem. Commun.* **1983**, 414. (b) For the oxidative addition of H_2 to $[\text{Ir}(\text{cod})(\text{diop})](\text{PF}_6)$, only one set of hydride resonances was discernible. Presumably the diastereomers were not resolved. Crabtree, R. H.; Felkin, H.; Fillebeen-Khan, T.; Morris, G. E. *J. Organomet. Chem.* **1979**, *168*, 183.

Stepwise Metal-Assisted Conversion of CSe_2 to Se_2 and CO_2 . Novel Bonding Mode of the Diselenium Molecule in the Double- Se_2 -Bridged Complex $[(\text{triphos})\text{Rh}(\mu\text{-Se}_2)_2\text{Rh}(\text{triphos})](\text{BPh}_4)_2\cdot 2\text{DMF}$

Claudio Bianchini,* Carlo Mealli, Andrea Meli, and Michal Sabat

Istituto per lo Studio della Stereochimica ed Energetica dei Composti di Coordinazione C.N.R., 50132 Firenze, Italy

Received February 26, 1985

Despite the academic, biological, catalytic, and synthetic interest in metal complexes containing chalcogens in their framework, surprisingly little is still known about the organometallic and coordination chemistry of CSe_2 . Only very recent studies have revealed the potentially enormous reaction possibilities of CSe_2 complexes.¹ In this paper we report an unprecedented metal-promoted transformation of $\eta^2\text{-CSe}_2$ into $\eta^2\text{-Se}_2$ via $\eta^1\text{-Se}_2\text{CPEt}_3$ and $\eta^2\text{-Se}_2\text{CO}$ intermediates (Scheme I).

It is well-known that, with adoption of the $\eta^2\text{-C-S}$ coordination mode, the electrophilicity of the carbon atom of the sulfur analogue of CSe_2 , CS_2 , is enhanced thereby facilitating attack of a nucleophile.² Accordingly, we have found that PEt_3 reacts with $(\text{triphos})\text{RhCl}(\eta^2\text{-CSe}_2)^{16}$ (**1**) in CH_2Cl_2 to give green crystals of the phosphoniodiselenocarboxylate complex $(\text{triphos})\text{RhCl}(\text{Se}_2\text{CPEt}_3)^3$ (**2**) (yield 70%). The latter complex reacts immediately at room temperature in CH_2Cl_2 solution with dioxygen to give OPEt_3 and yellow crystals of $(\text{triphos})\text{RhCl}(\text{Se}_2\text{CO})^5$ (**3**) (yield 60%), the first example of a diselenocarbonate complex. The diselenocarbonate complex **3** is obtained also by simple exposure in air either of solid samples or of solutions of **2**. In this case, however, OPEt_3 cannot be collected as it is sensitive to moisture.

The chloride ligand in **3** is easily replaced by other monofunctional ligands like N_3^- , but can be also definitely removed from the complex by treatment of solutions of **3** with NaBPh_4 in ethanol. As a result, the 16-electron rhodium(III) complex $[(\text{triphos})\text{Rh}(\text{Se}_2\text{CO})]\text{BPh}_4^6$ (**4**) is quantitatively obtained. A preliminary X-ray crystal-structure determination⁷ has shown that the diselenocarbonate ligand chelates the rhodium atom through both selenium donors with the oxygen atom remaining uncoordinated.

By bubbling molecular oxygen into a CH_2Cl_2 solution of **4** for 5 min, brown crystals of $[(\text{triphos})\text{Rh}(\mu\text{-Se}_2)_2\text{Rh}(\text{triphos})](\text{BPh}_4)_2$ (**5**) are precipitated in 60% yield, whereas CO_2 is evolved (Scheme I). Crystals of **5**·2DMF suitable for an X-ray analysis are obtained by recrystallizing **5** from DMF/butanol. Alternatively, compound **5** can be synthesized either by exposure in air of solutions of the diselenocarbonate **4** or by treatment of solutions of **4** with H_2O_2 . In the latter case, the reaction is immediate and it is possible to

(1) (a) Clark, G. R.; Grundy, K. R.; Harris, R. O.; James, S. M.; Roper, W. R. *J. Organomet. Chem.* **1975**, *90*, C37. (b) Roper, W. R.; Town, K. G. *Ibid.* **1983**, *252*, C97. (c) Werner, H.; Ebner, M. *Ibid.* **1983**, *258*, C52. (d) Werner, H.; Kolb, O. *Ibid.* **1984**, *268*, 49. (e) Bianchini, C.; Mealli, C.; Meli, A.; Sabat, M. *J. Chem. Soc., Chem. Commun.* **1984**, 1647.

(2) Yanoff, P. V. *Coord. Chem. Rev.* **1977**, *23*, 183.

(3) IR (Nujol mulls) 1030 (C-CH₃ rocking PEt_3), 970 cm^{-1} $\nu(\text{C}=\text{Se})$; $^{31}\text{P}\{^1\text{H}\}$ NMR (CD_2Cl_2 , 20 °C, 32.2 MHz) 30.45 (d, $J_{\text{PP}} = 17.2$, $J_{\text{PRh}} = 127.6$ Hz, triphos), 23.9 ppm (m, PCSe_2). This pattern does not vary with the temperature and is consistent with triphos acting as a tridentate ligand in five-coordinate complexes.⁴ The phosphoniodiselenocarboxylate ligand in **2** is monodentate probably to avoid a supersaturated 20-electron species. This is demonstrated by the existence of the complex $[(\text{triphos})\text{Rh}(\eta^2\text{-Se}_2\text{CPEt}_3)]\text{BPh}_4$ obtained by chloride ion abstraction from **2**.

(4) Bianchini, C.; Mealli, C.; Meli, A.; Sabat, M. *Inorg. Chem.* **1984**, *23*, 4125.

(5) IR (Nujol mulls) 1050 cm^{-1} $\nu(\text{CO})$; $^{31}\text{P}\{^1\text{H}\}$ NMR (CD_2Cl_2 , 20 °C, 32.2 MHz) 25.85 (t, $J_{\text{PP}} = 27$, $J_{\text{PRh}} = 108.1$ Hz), -6.24 ppm (d).

(6) IR (Nujol mulls) 1080 cm^{-1} $\nu(\text{CO})$; $^{31}\text{P}\{^1\text{H}\}$ NMR (CD_2Cl_2 , 20 °C, 32.2 MHz) 34.15 ppm (s, $J_{\text{PRh}} = 98.3$ Hz).

(7) Bianchini, C.; Mealli, C.; Meli, A.; Sabat, M. *J. Chem. Soc., Chem. Commun.*, submitted for publication.